



11th Canadian Masonry Symposium, Toronto, Ontario, May 31- June 3, 2009

REINFORCED CLAY MASONRY WALLS UNDER SHEAR-COMPRESSION LOADS: EXPERIMENTAL BEHAVIOUR

F. da Porto¹, F. Mosele² and C. Modena³

¹Assistant Professor, ² Ph.D. Candidate, ³Full Professor

Department of Structural and Transportation Engineering, University of Padova, Italy
daporto@dic.unipd.it, mosele@dic.unipd.it, modena@dic.unipd.it

ABSTRACT

In the framework of the DISWall project, funded by the European Commission, innovative construction systems for reinforced masonry walls were developed for the application in seismic areas. In particular, a new reinforced masonry system made with horizontally perforated clay units was developed on purpose for typical low-rise residential buildings to withstand in-plane actions. Thirty specimens of this type of masonry were characterized by means of uniaxial tests and by means of in-plane cyclic shear compression tests. The tests were carried out on either specimens with horizontal rebar reinforcement or truss reinforcement. Furthermore, the in-plane cyclic tests were carried out on both slender and squat specimens, under different pre-compression levels, in order to force both flexural and shear failure mechanisms. In the present contribution, the results of the cyclic tests carried out are discussed. Data of steel strain on rebars and trusses, ductility parameters, energy dissipation, stiffness degradation are discussed.

KEYWORDS: reinforced masonry; in-plane cyclic tests; strength; steel strain; ductility; energy dissipation; stiffness degradation.

INTRODUCTION

Reinforced and confined masonry have been developed in order to exploit the strength potential of masonry and solve its lack of tensile strength, improving significantly not only the resistance, but also the ductility and the energy dissipation capacity, that is the seismic behaviour, of the masonry walls [1; 2]. In the last decades, a large variety of reinforced and confined masonry techniques have been developed. The different masonry systems depend on many parameters: geometric shape and material of the units, composition of the mortar and/or grout, quantity and layout of the reinforcement [1]. In the following, the behaviour of a newly developed reinforced masonry system, made with horizontally perforated clay units, is described. Strength and ductility parameters are given. The effect of reinforcement in terms of strain and reinforcement type is discussed. Energy dissipation capacity, stiffness degradation, effect of aspect ratio and of applied axial load are also considered. The comparison with performance of walls with only horizontal reinforcement is carried out.

REINFORCED MASONRY SYSTEM

The tested reinforced masonry system is based on the use of concentrated reinforcement. On purpose horizontally perforated clay units are used in the masonry panel. They have recesses on the bed faces for placing the horizontal reinforcement (see Figure 1, left). Ordinary commercial units, 300 mm wide, with vertical holes are used to build the confining columns. Steel bars are used for vertical reinforcement, whereas for horizontal reinforcement, either steel rebars or prefabricated steel trusses can be adopted. The mortar has been expressly developed for this reinforced masonry system, in particular for what concern the properties of consistence, plasticity, and workability, to allow for a proper bed joint and recess filling. At the same time, the mortar has been developed to be used as proper filling of the reinforced vertical cavities. A complete description of the system is given in [3; 4].

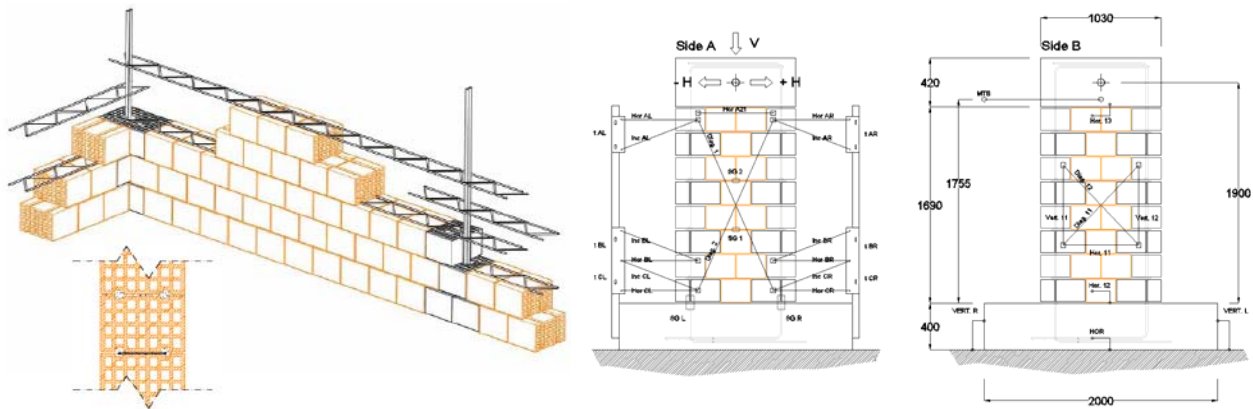


Figure 1: Construction systems based on the use of horizontally perforated clay units (left); slender specimens for in-plane cyclic testing (right).

EXPERIMENTAL PROGRAM

The main objective of the testing program was to assess the behaviour under in-plane cyclic actions of this kind of reinforced masonry wall system. The tests were repeated on two series of specimens, with different horizontal reinforcement. One series was built with usual steel rebars (specimens named SR), the other with prefabricated truss reinforcement (specimens named TR). In all of the specimens, the horizontal reinforcement was distributed on the specimens every other course. Specimens built with the entire reinforced masonry system and masonry panels without the confining columns (“H”) were tested under in-plane cyclic shear compression tests. One test was carried out on a specimen (“HSa”) with no vertical neither horizontal reinforcement, in order to check the behaviour of plain masonry. The shear compression tests on the entire reinforced masonry system were carried out on specimens characterized by two slenderness ratio, in order to force the shear behaviour (slenderness ratio “a” equal to 1.09) and the flexural behaviour (slenderness ratio “b” equal to 1.64, see Figure 1, right). The vertical reinforcement was constituted by two rebars with diameter of 16 mm at each masonry edge for squat specimen “a”, and by one rebar with diameter of 16 mm at each masonry edge for slender specimens “b”. Table 1 gives the test matrix for the in-plane cyclic shear-compression tests carried out. Tests on materials (mortar, units and reinforcement) and tests for the characterization of the compressive behaviour of masonry preceded the in-plane shear-compression tests. Their results are reported elsewhere [3; 4].

Table 1: In-plane cyclic shear-compression tests matrix

Series	N° of specimens	Dimensions (mm)	Vertical Reinf.	Vertical Renf. ratio	Horizontal Reinf.	Horizontal Renf. ratio
HS	2	1550x300x1690	-	-	-	-
SRHS	2	1550x300x1690	-	-	2Φ6/400mm	0.045%
TRHS	2	1550x300x1690	-	-	1truss/400mm	0.040%
SRSa	2	1550x300x1690	4Φ16	0.172%	2Φ6/400mm	0.045%
TRSa	2	1550x300x1690	4Φ16	0.172%	1truss/400mm	0.040%
SRSb	2	1030x300x1690	2Φ16	0.130%	2Φ6/400mm	0.045%
TRsb	2	1030x300x1690	2Φ16	0.130%	1truss/400mm	0.040%

The specimens were tested with cantilever type boundary condition, with fixed base and top end free to rotate, by applying a centred and constant vertical load equal to 11% and 16% of the measured maximum compressive strength of the RM system walls, and corresponding to 15% and 22% of the measured maximum compressive strength of the walls without confining columns. The corresponding compressive stress levels (0.4 and 0.6 N/mm²) are adequate to represent the typical vertical loads for two up to four-storey height buildings. Two specimens, one for each pre-compression level, constitute each series reported in Table 1.

The specimens were instrumented with 24 potentiometers to measure deformations and displacements and 4 strain-gauges to measure strains in the reinforcement at characteristic sections of the wall (see Figure 1, right). Horizontal cyclic displacements, with increasing amplitude and with peaks repeated three times for each displacement amplitude, were applied at a frequency of 0.004 Hz. The displacement history was determined by fixing a reference critical displacement $\delta_{cr}=3-5.5$ mm (inter-storey drift equal to 0.17%-0.30%, as in [5]) and considering that the first non linearity is expected for displacements equal to 1-1.5mm (inter-storey drift between 0.05%-0.08%), as observed in previous experimental tests [6-8].

LOADS AND DISPLACEMENTS

During experimental tests the attainment of four limit states, which can be used to idealize the masonry wall behaviour, can be observed. The limit states correspond to changes in how the specimens resist at the progressive increment of applied lateral displacement. The flexural cracking limit (H_f, δ_f) was related to the occurrence of the first flexural crack on the horizontal joints. The crack limit state (H_{cr}, δ_{cr}) was fixed in correspondence of the second main non-linearity, on the load-displacement diagrams. This occurred when the first significant diagonally oriented shear crack appeared on squat walls, with simultaneous discontinuity on strains measured on horizontal rebars. It corresponded to the yielding of vertical reinforcement for slender specimens. The third limit state was related to the attainment of the maximum resistance H_{max} , at a corresponding displacement level δ_{Hmax} , whereas the fourth limit state occurred when the maximum displacement δ_{max} was reached, to which a consequent value of residual lateral resistance H_{dmax} corresponds. This limit state was fixed at the displacement level at which the last stable cycles occurred. This idealization, developed on purpose for plain masonry [9], was thus adapted to the tested reinforced masonry wall specimens.

Detailed information is given elsewhere [4]; Table 2 summarizes failure modes, maximum loads and maximum displacements, load and ductility ratios.

Table 2: Failure modes; maximum loads and displacements; load and ductility ratios

Specimen	Failure Mode	H _{max} (kN)	δ _{max} (mm)	H _{cr} /H _{max}	H _{dmax} /H _{max}	H _{dmax} /H _{cr}	δ _{cr} /δ _{Hmax}	δ _{max} /δ _{Hmax}	δ _{max} /δ _{cr}
$\sigma_0 = 0,6 \text{ N/mm}^2$									
HS 0.6	Flex	77	35.00	0.86	0.63	0.73	0.31	2.00	6.50
TRHS 0.6	Flex	106	15.01	0.89	0.81	0.91	0.32	1.21	3.74
SRHS 0.6	Flex	114	30.01	0.80	0.89	1.12	0.19	1.28	6.64
TRSa 0.6	Shear	211	12.51	0.76	0.89	1.16	0.41	1.03	2.50
SRSa 0.6	Shear	218	15.01	0.72	0.89	1.24	0.40	1.22	3.00
TR Sb 0.6	Flex	93	45.00	0.92	0.81	0.87	0.54	2.16	4.00
SRSb 0.6	Flex	90	30.00	0.89	0.47	0.53	0.42	1.42	3.42
Average	-	-	-	0.83	0.77	0.94	0.37	1.47	4.26
$\sigma_0 = 0,4 \text{ N/mm}^2$									
HS 0.4	Flex	77	32.49	0.86	0.84	0.98	0.18	1.54	8.34
TRHS 0.4	Flex	79	64.98	0.92	0.47	0.51	0.23	2.66	11.54
SRHS 0.4	Flex	81	59.99	0.89	0.32	0.36	0.12	1.55	12.63
TRSa 0.4	S/F	201	19.99	0.71	0.83	1.17	0.35	1.50	4.33
SRSa 0.4	S/F	201	19.99	0.71	0.86	1.20	0.33	1.16	3.56
TR Sb 0.4	Flex	81	79.87	0.91	0.36	0.39	0.50	3.33	6.63
SRSb 0.4	Flex	79	64.99	0.87	0.29	0.33	0.35	2.43	6.88
Average	-	-	-	0.84	0.57	0.71	0.30	2.02	7.70

STRAINS ON REINFORCEMENT

The horizontal reinforcement, instrumented with strain-gauges, acts in tension when subjected to lateral loads, as expected. For the squat specimens, the horizontal reinforcement is characterized by an initial phase with strain almost null and by a sudden increase of strain when the first relevant diagonal crack opens (see Figure 2a and b). These diagrams give the load-displacement envelop curve in term of the identified limit states and the contribution of horizontal reinforcement in terms of strain (right vertical axes) and of load (left vertical axis). Following, the shear reinforcement strain gradually increases, also after the attainment of maximum load, although it does not reach yielding. These data thus confirm that horizontal reinforcement keeps together the cracked parts of the wall [1]. As the reinforcement avoids crack to widen, new uniformly distributed cracks open. The horizontal reinforcement strain (and the corresponding load) in the slender specimens is generally smaller than in the squat ones (see Figure 2c and d). For the slender specimens, the contribution of horizontal reinforcement seems to be more important in the post-peak phase, probably providing a positive stability effect. It is to note that in both cases (squat and slender specimens) the truss reinforcement (TRS) is characterized by higher strain than the rebars (SRS). However, for squat walls, considering the smaller resistant area of the truss, this results in a comparable contribution in terms of load. The strain-gauges installed on the horizontal reinforcement of walls without vertical reinforcement (TRHS and SRHS) confirmed the substantial ineffectiveness of horizontal reinforcement, on walls without vertical reinforcement. The various axial load levels did not have a clear influence on the attainment of crack limit for the squat specimens besides for TRSa, where with lower pre-compression, the strain was activated at smaller displacements (see Figure 2a and b). On the slender specimens, the different axial load level affected the shear reinforcement strain, since for lower pre-compression, the horizontal reinforcement started working when the maximum capacity is reached (see Figure 2c and d), whereas for higher pre-compression, strains gradually increased from the initial phases of the test.

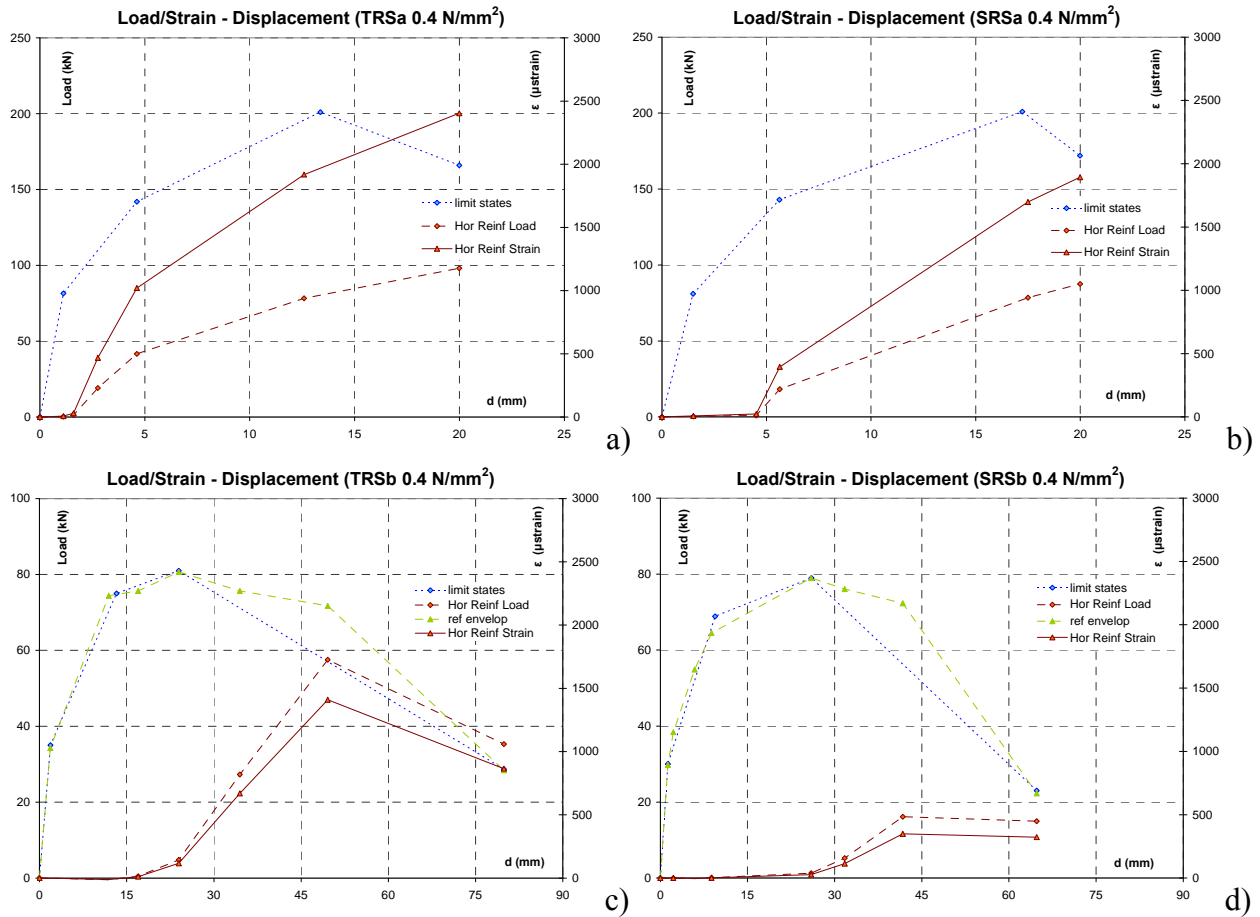


Figure 2: Load-displacement envelop curves and strains and loads in horizontal reinforcement: squat and slender walls with truss (a; c) and rebars (b; d)

Vertical reinforcement, when the wall is subjected to reversals lateral load, alternates between tension and compression strains. As for reinforced concrete, the strain in compression is small, whereas that in tension is significant. Vertical strains are activated by the first flexural crack and they reach yielding just before the attainment of maximum load, when also crushing of units occurs. Compression strain remains small also due to buckling, which induces a combined compressive and bending stress into the bar during the compression phase and reduces the tension strains measured during the tension phase.

For squat walls, the tensile strains on vertical reinforcement increase with the applied lateral load almost with linear trend, starting from the first phases of the test (see Figure 3a and b). The vertical reinforcement reaches yielding strain at displacements of about 9-10 mm, and lateral loads of 190-200 kN, at the displacement step before the attainment of the maximum load. The loss of tensile strain following yielding is related to the buckling effect. In slender walls, the initial trend of strains in vertical reinforcement is similar to that of squat walls. Yielding is reached at displacements of 10-11 mm, and lateral loads of 75-71 kN (see Figure 3c and d). Yielding in this case deeply changes the response of the wall. Also in this case, after the attainment of values of 6000 μstrain , strains decrease due to the buckling effect.

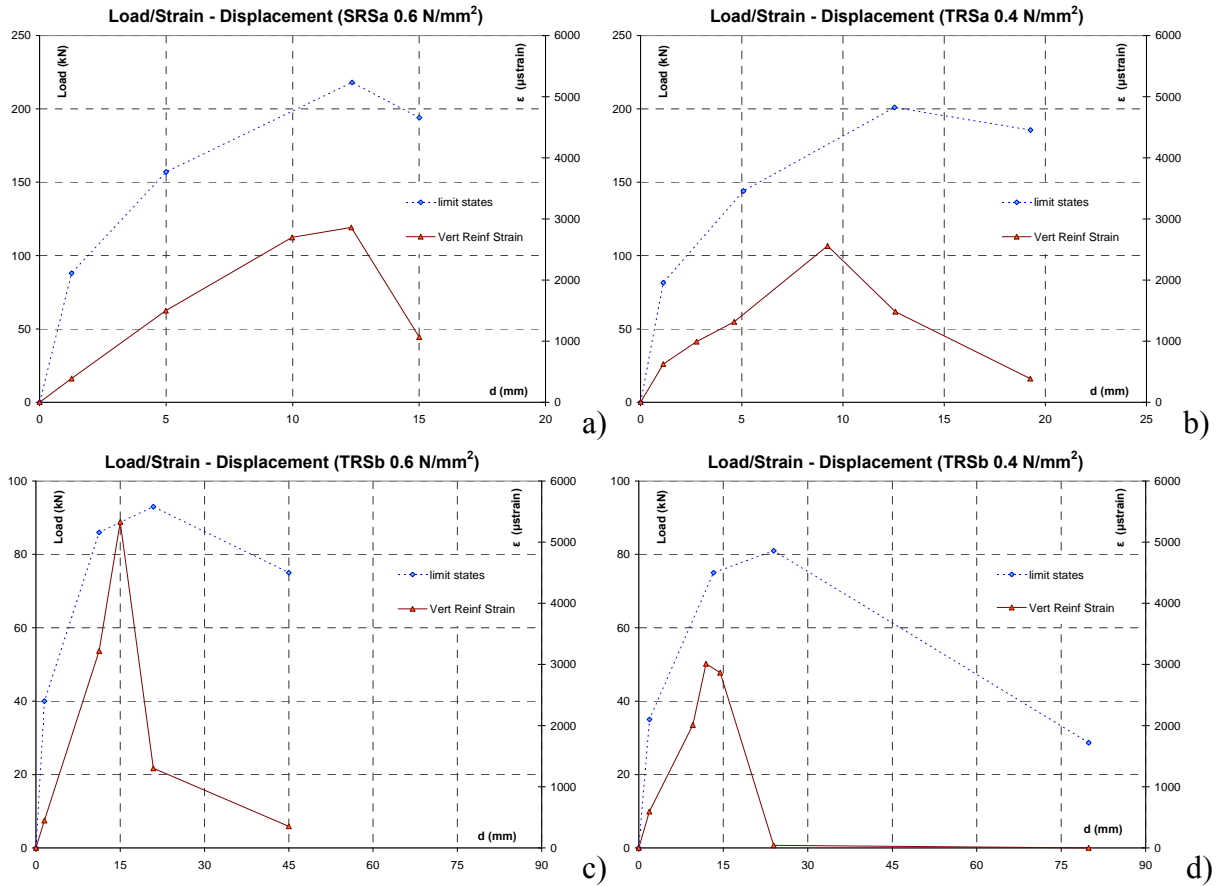


Figure 3: Load-displacement envelop curves and strains and loads in vertical reinforcement: squat walls under two axial load level (a; b) and slender walls (c; d).

EFFECT OF AXIAL LOAD

As expected, the increase of axial load allows increasing the lateral load capacity, although it induces a decrease of ductility and a possible change of failure mechanism, since the increment of shear and flexural strength is not proportional (see Table 2).

The slender specimens (SRSb and TRSb) were characterized by an average increment of strength of 15%, independently by different shear reinforcement type, with clear flexural failure mechanism. The average strength increment for squat specimens (SRSa and TRSa) was 6%, which is less than that of slender specimens since the shear failure mechanism is less affected by the amount of axial load. For the specimens without vertical reinforcement (SRHS and TRHS) the average strength increment was 38%. This is higher than in RM specimens, since the percentage ratio of applied axial load to masonry compressive strength is higher. Moreover, in this case axial load is the only parameter that affects flexural strength, whereas the presence of vertical reinforcement in the RM specimens decreases, in percentage, the influence of the axial load. The increase of axial load generally implies, for both slender and squat specimens, small decrease of the $\delta_{H_{max}}/\delta_{cr}$ ratio and a significant decrease of the δ_{max}/δ_{cr} ratio (see Table 2). The improvement of ductility, for reduced axial load, is related to the lengthening of post-peak phase. In the squat specimens, the increase of axial load also changes the behaviour from a relatively

ductile and mixed flexural/shear mode to a brittle shear mode, as already observed by various researches such as [10]. In the first, a marked deterioration of the compressive toe due to the buckling of the vertical rebars was observed, whereas in the latter, shear failure characterized by a well defined diagonal compression strut, with cracks passing through the joints and the units, was more evident. For slender specimens, the failure mechanism is always flexural, therefore the attained ductility is higher than that of squat specimens (from 35% to 71%; see Table 2). The higher pre-compression level led to crushing of the compressed toe with yielding of the tensile reinforcement, whereas yielding and subsequent tension failure of reinforcement occurred for lower pre-compression level. The failure thus developed across the border between fields 2 and 3, usually adopted for flexural design of reinforced concrete.

Energy dissipation capacity in the RM specimens was lower than usually reported for reinforced masonry walls [8; 11], although it is higher of what commonly reported for unreinforced masonry [6]. The variation of axial load induces an increase of total dissipated energy for both squat and slender specimens, due to the increased ultimate displacement reached. In any case, the trend of the ratio between dissipated and input energy during the tests is independent by the investigated axial load levels (Figure 4). Only on TRSb specimens, the pre-compression level seems to have some influence on energy dissipation, where the higher the pre-compression, the lower the dissipated energy. The variation of axial load does not influence significantly also stiffness degradation, as represented in Figure 5, and viscous damping coefficient.

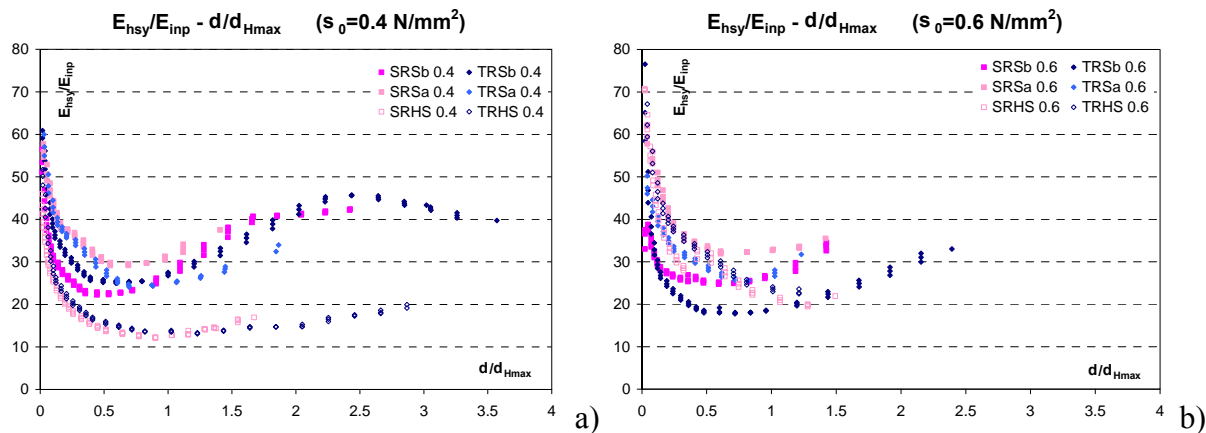


Figure 4: Dissipated/Input energy vs normalized displacement: 0.4 N/mm^2 (a) and 0.6 N/mm^2 (b).

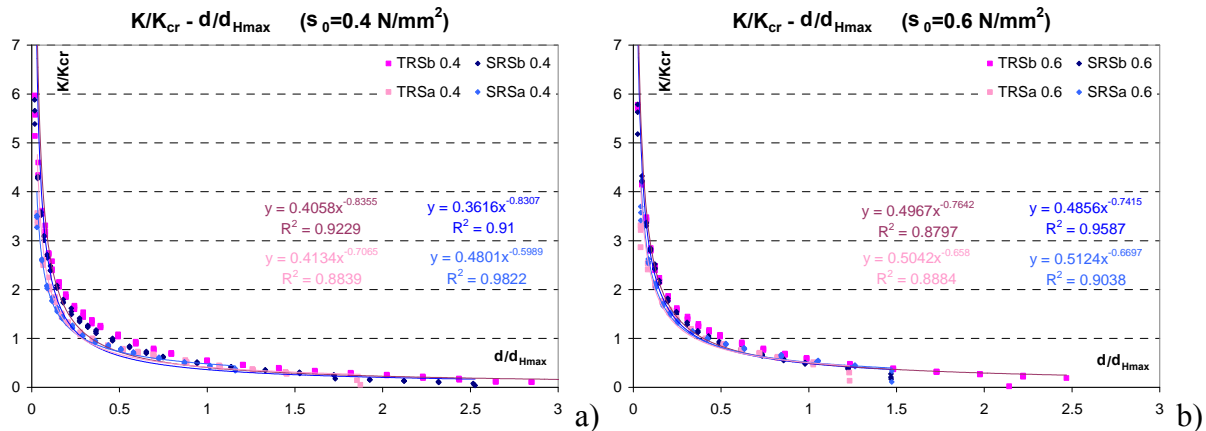


Figure 5: Stiffness degradation vs normalized displacement: 0.4 N/mm^2 (a) and 0.6 N/mm^2 (b).

EFFECT OF ASPECT RATIO

As expected, the main effect of aspect ratio is that slender specimens ($h/l=1.64$) are dominated by flexural failure mode, whereas the squat ones ($h/l=1.09$) by shear failure mode. The increase of slenderness leads necessarily towards flexural failure, since it induces a reduction of flexural strength which is higher than the reduction of shear strength. The various type of failure mechanisms, due to the aspect ratio, are characterized by high strength and reduced displacement capacity for the shear one and by lower strength with higher displacement capacity for the flexural mechanism (see Table 2). The higher ductility of slender walls is concentrated in the post-peak phase, whereas the ductility ratio $\delta_{Hmax}/\delta_{cr}$ is smaller for slender than for squat specimens, since cracking in the latter occurs earlier than yielding in the previous.

The ratio between dissipated and absorbed energy (and viscous damping coefficient, too) in squat specimens is higher, at equal displacements, than that of slender specimens, but the latter can overall dissipate higher quantity of energy thanks to the higher displacement capacity (Figure 4). The stiffness degradation, referred to normalized displacement, is almost the same for squat and slender specimens (Figure 5).

EFFECT OF THE TYPE OF REINFORCEMENT

The effect of the different type of horizontal reinforcement was non influential in terms of strength (Table 2) and stiffness degradation (Figure 5). The displacement capacity of truss reinforced masonry walls (δ_{max}) is generally equal or higher than that of walls reinforced with rebars. Related to the different cracking limit states, in some cases, ductility (ratio δ_{max}/δ_{cr}) is higher with truss reinforcement, in some others, it is not. However, values related to similar TRS and SRS specimens (same aspect ratio and applied axial load) are always in the same ranges (Table 2). In this sense, it seems that the strength of the units placed at the compressed toe is influencing the collapse more than the different adopted reinforcements.

The ratio of dissipated to input energy is slightly higher for SRS specimens independently by pre-compression load and aspect ratio (Figure 4). This can be related to strain of horizontal reinforcement (Figure 2). As already observed, the truss reinforcement reaches higher strain than rebars. This means wider shear cracks in the case of truss horizontal reinforcement, which reduce the energy dissipation due to lack of friction along the crack.

From the experimental observations, it was noted that both types of horizontal reinforcement, which were bended around the vertical reinforcement at the vertical edges of the walls, could not prevent buckling of vertical rebars. However, in the specimens without vertical reinforcement (TRHS and SRHS) and highest axial load applied, whereas SRHS failed with localized crushing of the compressed toe at just one edge, TRHS collapsed when the first two courses of units were crushed, with transversal deformation of the truss, which demonstrates some positive contribution, in terms of confining effect, of the truss. This confining effect on the compressed zones of the walls was proved also for the slender walls, related to the flexural failure. In any case this effect had no influence on the mechanical properties of the masonry walls.

COMPARISON BETWEEN MASONRY WITHOUT VERTICAL REINFORCEMENT AND COMPLETE REINFORCED MASONRY SYSTEM

The comparison between squat specimens without vertical reinforcement (HS series) and made with the complete RM system (Sa series), shows that the strength of the entire RM system is twice than that of HS specimens. The displacement and rotation angle at the crack limit state is

similar for the two series; but at maximum resistance and maximum displacement those of the HS series are higher than those of the Sa series, because the HS series is characterized by rocking. Ductility of Sa series is thus lower (see Table 2). Rocking effect does not allow completely exploiting the wall capacity, in term of both strength and energy dissipation.

The ratio of dissipated/input energy shows different behaviour according to the axial load level. For the higher pre-compression load, the ratio is quite similar during the first phases of the test, for specimens without vertical reinforcement (TRHS and SRHS) and for RM specimens. After the crack limit state, the RM walls are able to maintain the dissipation capacity, whereas the specimens without complete reinforcement show a decrease of that ratio. For lower pre-compression level RM specimens dissipate higher quantity of energy than TRHS and SRHS specimens during each phase of test (Figure 5). In this case, despite they have horizontal reinforcement, they dissipate an amount of energy that is close to that of unreinforced masonry (around 10%). The same considerations are valid for viscous damping coefficient. The stiffness degradation of walls without vertical reinforcement is slightly higher than that of RM walls.

CONCLUSIONS

The discussion of the experimental results indicates that, in regards the variation of axial load, its increase enhances the shear capacity at the expenses of displacement capacity, particularly in the post-peak phase, thus of ductility. The variation of axial load allows controlling the failure mode: from brittle shear failure to ductile mixed shear/flexural failure, and from less to more ductile flexural failure. However, it does not affect significantly stiffness degradation, the ratio of dissipated/input energy, and the viscous damping coefficient, although this conclusion is drawn from very limited axial load range.

Regarding the aspect ratio, the higher it is (slender RM specimens), the higher ductility is, where the displacement capacity concentrates in post-peak phase. However, squat RM specimens have higher ratio of dissipated/input energy and higher viscous damping coefficient than slender walls, independently by axial load level. On the contrary, the aspect ratio does not influence stiffness degradation, in relation to normalized displacement (ratio of current displacement to displacement at maximum load).

The difference in ductility due to the different types of horizontal is not so marked, even though truss reinforcement generally provides equal or higher displacement capacity. On the other hand, truss reinforcement dissipates less energy than rebars, at equal displacement. These two characteristics balance each other; therefore, the global energy balance can be similar. Truss reinforcement activates some confining effect in the compression zone generated by flexure, but does not influence the overall mechanical characteristic of walls, or stabilize the failure process at higher axial load level. In this case, stiffness degradation is also not affected by the different type of horizontal reinforcement.

The presence of vertical reinforcement, that makes the RM system complete, doubles the shear capacity of the walls, but to a certain extent decreases the ductility, as walls without vertical reinforcement are affected by rocking and thus reaches higher ultimate displacements. The RM walls have, obviously, higher energy dissipation capacity. However, this is evident for lower axial load levels, whereas for higher values of axial loads, the presence of only horizontal reinforcement is already able to give some energy dissipation capacity, and the ratio of dissipated to input energy of RM specimens increases only after the crack limit state. In this case, stiffness degradation, in relation to normalized displacement, is higher for the walls without vertical reinforcement (TRHS and SRHS).

Some of these observations confirm that phenomena observed in previous experimental tests, which were carried out on reinforced masonry walls with vertically perforated clay units, are still valid when horizontally perforated units with concentrated reinforcement are used. It is shown that truss reinforcement can be adequately used in place of usual rebars, and the differences found in these tests are related to the slightly lower cross sectional area of the truss, compared to the two rebars. Furthermore, some new insight is given to the dependency of meaningful parameters, such as energy dissipation or stiffness degradation, to varying ‘boundary’ conditions such as level of applied axial load and aspect ratio, and to the effectiveness of a complete RM system compared to partially reinforced walls.

ACKNOWLEDGEMENTS

The present work is being carried out under the framework of the European Contract COOP-CT-2005-018120: ‘Developing Innovative Systems for Reinforced Masonry Walls - DISWall’. The enterprises involved in the production of the described system, Laterizi Alan Metauro s.r.l. and Tassullo S.p.A. (Italy), Bekaert SA/NV (Belgium) are partners of the research projects.

REFERENCES

1. Tomažević, M., “Earthquake-resistant design of masonry buildings”, Imperial College Press, London, 1999
2. Tassios, T.P., (1988), “Meccanica delle murature”, Liguori Editore, Napoli, Italy, (in italian).
3. Mosele F., da Porto F., Dalla Benetta M., Modena C. (2008) “Experimental behaviour of newly developed system for load bearing reinforced masonry walls” 14th International Brick and Block Masonry Conference, Sydney, Australia, on CD-ROM
4. Mosele F. (2009) “In-plane and out-of-plane cyclic behaviour of reinforced masonry walls”. PhD thesis, University of Trento, February 2009
5. Tomažević, M., Lutman, M., (1997), “Influence of reinforcement and block strength on seismic behaviour of reinforced masonry walls”, Proc. 11th Int. Brick/Block Masonry Conf., October 14-16, 1997, Tongji University, Shanghai, China, pp.217-226.
6. da Porto, F., Grendene, M., Modena, C. (2009) “Estimation of load reduction factors for clay masonry walls”, accepted for publication on Earthquake Engineering and Structural Dynamics, John Wiley & Sons, Ltd; DOI: 10.1002/eqe
7. Magenes, G., Calvi, G.M., Gaia, (1996), “Shear tests on reinforced masonry walls”, Rapporto RS-03/96, Dip. Di Meccanica Strutturale, Università degli Studi di Pavia, Marzo 1996, (in italian)
8. Lucchetta, S., Zanconato, M., (1994), “Valutazione sperimentale e modellazione del comportamento di pannelli in muratura armata sollecitati nel proprio piano”, Tesi di Laurea, Università degli Studi di Padova, A.A. 1993/1994, (in Italian).
9. Abrams, D.P. (2001) “Performance based engineering concepts for unreinforced masonry building structures” Prog. Struct. Engng. Mater.; John Wiley & Sons, 3:48-56. 2001
10. Shing, P.B., Schuller, M., Hoskere, V.S., (1990), “In plane resistance of reinforced masonry shear walls”, Journal of Structural Engineering, ASCE, Vol.116, No. 3, March, 1990, pp.619-640.
11. Tomažević, M., Lutman, M., Petković, L., (1996), “Seismic behaviour of masonry walls: Experimental simulation”, Journal of Structural Engineering, ASCE, Vol.122, No. 9, September, 1996, pp.1040-1047.